water

MDPI

Article

Hydrochemical Characteristics and Genesis of Sand–Gravel Brine Deposits in the Mahai Basin of the Northern Qinghai–Tibetan Plateau

Hongkui Bai [1,2], Tong Pan [3,*], Guang Han [1,2,*], Qishun Fan [4,5], Qing Miao [1,2] and Haiyi Bu [1]

[1] Qaidam Comprehensive Geological and Mineral Exploration Institute of Qinghai Province, Golmud 816099, China; 18935591981@163.com (H.B.); qmiao_hgu@163.com (Q.M.); 13369793462@163.com (H.B.)
[2] Qinghai Provincial Key Laboratory of Exploration and Research of Salt Lake Resources in Qaidam Basin, Golmud 816099, China
[3] Qinghai Geological and Mineral Exploration and Development Bureau, Xining 810008, China
[4] Key Laboratory of Green and High-End Utilization of Salt Lake Resources, Qinghai Institute of Salt Lakes, Chinese Academy of Sciences, Xining 810008, China; qsfan@isl.ac.cn
[5] Qinghai Provincial Key Laboratory of Geology and Environment of Salt Lakes, Xining 810008, China
* Correspondence: pant66@163.com (T.P.); hanguang23@mails.ucas.ac.cn (G.H.)

Abstract: The sand–gravel brine deposit in the Mahai Basin is a newly discovered large-scale potassium–bearing brine deposit. The potassium–bearing brine is primarily found at depths exceeding 150 m within the porous alluvial and fluvial sand–gravel reservoir of the Middle to Lower Pleistocene. This deposit is characterized by a relatively shallow water table, moderate–to–strong aquifer productivity, high salinity, and a KCl content that meets the conditions for exploitation, with the advantage of reduced salt crystallization during well mining, making it a potential reserve base for potash development. A geochemical analysis of the sand–gravel brine revealed consistent trends for the major ions K^+, Na^+, Mg^{2+}, Cl^-, and SO_4^{2-} along the east–west axis of the alluvial fan, while Ca^{2+} showed an opposite trend compared to Mg^{2+}. Along the exploration lines from north to south, the concentrations of the main ions gradually increase. The brine is enriched in Na^+ and Cl^- ions, while SO_4^{2-} and HCO_3^- are depleted. In the K^+-Na^+-Mg^{2+}/Cl^--H_2O (25 °C) quaternary phase diagram, the brine falls within the halite stability field, with the hydrochemical type classified as chloride type. The brine coefficient characteristics indicate a multi-source origin involving residual evaporation, salt rock leaching, and metamorphic sedimentary brine. Comparison studies of the ionic composition and isotopic signatures (δD, $\delta^{18}O$, $\delta^{37}Cl$, and δ^7Li) of deep sand–gravel brines in the study area with interstitial and confined brines in the southern depression suggest similar geochemical characteristics between them. The genetic analysis of the deposit proposes that during the basin tectonic evolution, the potassium-rich interstitial and confined brines originally located in the southern depression of the Mahai Basin were displaced under compressional forces and migrated northward as the depositional center shifted, eventually backfilling into the loose alluvial and fluvial sand and gravel reservoirs at the front of the Saishiteng Mountains, forming the deep sand–gravel brine deposits in the foreland.

Keywords: Mahai basin; sand–gravel brine deposit; hydrochemical characteristics; deposit genesis

check for updates

Citation: Bai, H.; Pan, T.; Han, G.; Fan, Q.; Miao, Q.; Bu, H. Hydrochemical Characteristics and Genesis of Sand–Gravel Brine Deposits in the Mahai Basin of the Northern Qinghai–Tibetan Plateau. *Water* **2024**, *16*, 3562. https://doi.org/10.3390/w16243562

Academic Editor: Kristine Walraevens

Received: 12 September 2024
Revised: 19 October 2024
Accepted: 21 November 2024
Published: 11 December 2024

Copyright: © 2024 by the authors. Licensee MDPI, Basel, Switzerland. This article is an open access article distributed under the terms and conditions of the Creative Commons Attribution (CC BY) license (https://creativecommons.org/licenses/by/4.0/).

1. Introduction

Potassium (K) is an indispensable component of agricultural fertilizer, playing a vital role in agricultural production and ensuring national food security [1]. Potash fertilizer consumption accounts for over 90% of the world's potassium salt production capacity, while other industrial sectors account for only about 10% [2]. In nature, K resources can be categorized into solid potassium salt resources (including soluble solid potassium salts and

insoluble solid potassium salts) and liquid potassium resources (involving underground brine and brine from Quaternary salt lakes) [3]. The Qaidam Basin (QB), located in the northern part of the Qinghai–Tibetan Plateau (QTP), is a Mesozoic–Cenozoic intermontane sedimentary basin rich in solid and liquid potassium salt resources [1,4]. Secondary basins containing solid and liquid potassium resources in the QB are the Mahai Basin, Dalangtan Depression, and Kunteyi Basin [4–6]. These areas are not only significant for research on continental potassium mineralization theory but also serve as crucial bases for the development and utilization of K resources in China [4].

In recent years, a series of deep brine deposits have been sequentially identified within the Dalangtan–Heibei, Chahansilatu, Kunteyi, and Mahai depressions in the western QB [2]. These brines are distinguished by their relatively high K content (0.31~1.56%) and significant reserves (350 million tons in KCl), making them prime candidates for future development and exploitation as K-bearing brine resources [2,5]. Recent scientific studies have been conducted on the geochemical characteristics, evolutionary paths in the Na^+-K^+-Mg^{2+}//Cl^--H_2O metastable phase diagram, evaporation experiments, distribution patterns, origin, and metallogenic model of sand–gravel brines in the western QB, using data from multiple boreholes [2,6–9]. The MHB, situated in the northern region of the QB, offers a highly suitable research site for an integrated investigation into the hydrochemical characteristics and formation process of sand–gravel brines owing to several compelling factors: (1) the sand–gravel brines in the MHB are characterized by relatively high K^+ (0.46–3.28 g/L) and substantial reserves (10 million tons in KCl) [2,8,9]. (2) In recent years, systematic geological exploration of sand–gravel brine resources has been conducted in the fore-mountain alluvial fan of Saishiteng Mountain in the MHB, resulting in the accumulation of a significant amount of data. (3) A wealth of research data and a well-developed theoretical framework have been accumulated for the potassium brine deposit in the MHB [4,8–13]. (4) Various water bodies in the MHB (including river water, groundwater, surface lake brines, intercrystalline brines, confined brines, and anticlinal structural brines) have been collected, providing materials for comparison and research.

Therefore, in this study, the major and trace elements of deep K-containing sand–gravel brines from 21 boreholes, including MH-0005, MH-0802, and MH-1609, in the MHB are systematically determined. The method of characteristic coefficient analysis, phase diagrams, and the salt-out law of brine are employed for systematic analysis. Moreover, the ion content and isotope (H, O, Cl, and Li) values of intercrystalline brines and confined brines in the southern depression of the MHB are gathered. We attempt to delineate the hydrochemical characteristics and origin of deep K-bearing sand–gravel brines in the MHB. This work is highly significant for enhancing our understanding of the hydrochemical characteristics and origin of the sand–gravel brines, as well as aids in directing the exploration breakthrough of similar brine deposits in the vicinity of the QB.

2. Geology Setting

The Qaidam Basin (QB), a vast, closed basin located on the northeastern edge of the Qinghai–Tibetan Plateau, is delimited by the Qilian Mountains to the north, the Kunlun Mountains to the south, and the Altyn Tagh Mountains to the west [14–18]. The Mahai Basin (MHB) (refer to Figure 1b), situated in the northern region of the QB, is a large integrated basin abundant in solid evaporites and brine resources [12]. Surrounded by the Saishiteng Mountain to the north, the Altyn Tagh Mountain to the northwest, the Lenghu anticline tectonic belt to the southwest, and the Nanbaxian anticline tectonic belt to the south, the MHB spans an area of 3700 km^2. Positioned as a subsidence zone in the northern QB, the sedimentary facies within the MHB predominantly feature alluvial fans, braided rivers, and lakes [19].

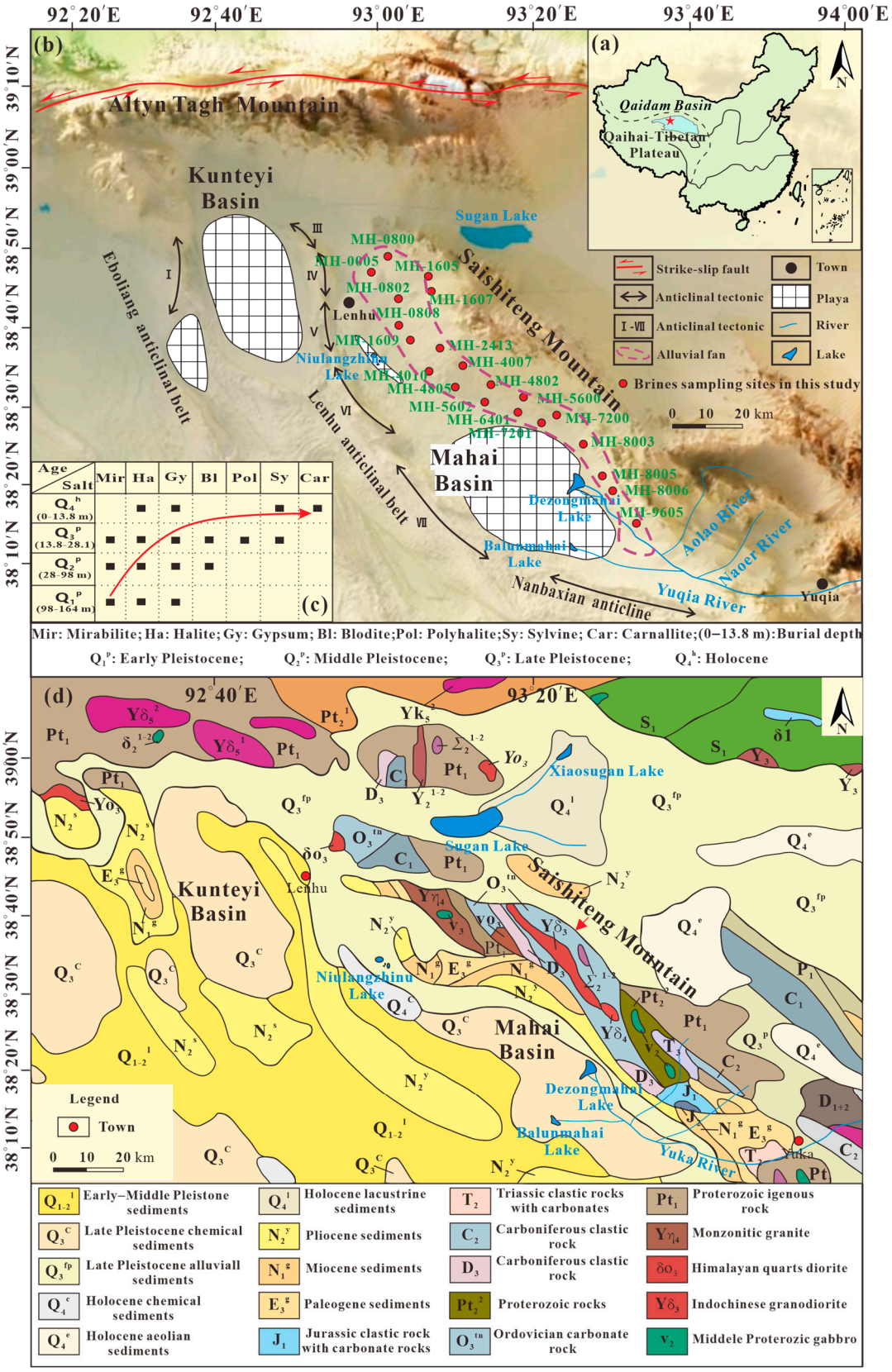


Figure 1. Geological and hydrologic settings and sampling locations in MHB: (**a**) the location of Qaidam Basin; (**b**) distribution map of MHB and sampling sites; (**c**) precipitation of Q_1^p to Q_4^h salt minerals in MHB; and (**d**) stratigraphic and lithological distribution of MHB and its surrounding area.

The MHB experiences an extremely arid climate, with an average annual precipitation of only 29.61 mm/year and an average potential evaporation of 3040 mm/year. This arid and cold climate, combined with its closed topography, shapes the unique geological environment, recharge, runoff, and groundwater discharge characteristics of the region [19,20]. The interaction of the surrounding mountain systems and anticlinal belt creates a sedimentary environment known as a "high mountain deep basin". The MHB is home to three salt lakes: Dezongmahai (DZMH) Lake, Balunmahai (BLMH) Lake in the eastern MHB, and Niulangzhinu (NLZV) Lake in the northwestern MHB (see Figure 1b). These salt lakes contain intercrystalline brines, lake surface brines, and evaporitic layers, collectively forming salt playa. The phreatic brine layer, which predominantly occurs within the Holocene halite layer at depths ranging from 0 to 18.52 m with an average depth of 0.43 m, is interpreted as intercrystalline brines [12]. The deep, confined brines in the MHB are stratified into three layers, primarily distributed below 18.5 m. The first confined brine layer lies in the upper Middle Pleistocene and lower Late Pleistocene, the second layer in the middle and lower Middle Pleistocene, and the third layer in the upper Early Pleistocene [12]. Sand–gravel brines are predominantly found in the alluvial fan at the front of Saishiteng Mountain, while anticlinal brines are concentrated in the LH anticlinal tectonic belt in the southern MHB [12]. Three hydrochemical types, namely Cl-SO_4, Ca-Cl, and Na-HCO_3-SO_4 types, are observed in the MHB. Intercrystalline brines are classified as Cl-SO_4 types, sand–gravel brines and anticlinal brines are Ca-Cl types, and the lake surface water system of the MHB, including the Yuqia River and its tributaries (Aolao River and Naoer River), belongs to the Na-HCO_3-SO_4 type [15,18,21,22]. Moreover, various salt minerals have been deposited in the MHB, such as halite, gypsum, calcite, potash salt, and dolomite (see Figure 1c).

The Quaternary strata in the MHB are extensive, with exposed strata containing materials from the Late Pleistocene, Early–Middle Pleistocene, and Holocene periods [19]. The anticlinal structures surrounding the basin are capped by the Upper Youshashan Formation (N_2^y) of the Neogene system, primarily consisting of shallow lacustrine gray mudstone, sandy mudstone, and some gypsum. Overlying the Saishiteng Mountain, the front strata include Late Pleistocene alluvial fan sediments, as well as the Neogene Upper Youshashan Formation (N_2^y), Upper Ganchaigou Formation (N_1^g), and Paleogene Lower Ganchaigou Formation (E_3^g). The alluvial fan at the base of Saishiteng Mountain serves as a key reservoir for sand–gravel brines, predominantly composed of gravel, medium-coarse sand, gravel sand with pebbles, and fine sand (Figure 2, Table S1). The lithology breakdown is as follows: the Upper Youshashan Formation (N_2^y) features shallow lacustrine gray mudstone, sandy mudstone, and some gypsum. The Upper Ganchaigou Formation (N_1^g) comprises semi-deep lacustrine sedimentary brown-red and gray-purple mudstone, sandy mudstone, and sandstone mixed with gray marl, occasionally charcoal mudstone. The Lower Ganchaigou Formation (E_3^g) consists of deep lacustrine facies with gray-purple-gray mudstone, brown-gray siltstone, argillaceous siltstone, and dark gray marl [7]. Generally, the Paleogene and Neogene Formations shape the landscape in and around the MHB [15].

The Saishiteng Mountain system is part of the northern margin tectonic belt of the QB. This mountain serves as the origin of sand, medium–fine sand, and fine sand in its frontal alluvial and diluvial fan, while also contributing salt–forming solutes to the salt lake of the Mahai Basin. The main geological formations in the area include the Paleoproterozoic Dakendaban Group and the Lower Paleozoic Tanjianshan Group, which are oriented in a NW or NNW direction [23,24]. The Dakendaban Group consists of volcanic–clastic rock assemblages with intermediate- to high-grade metamorphism [25,26], while the Tanjianshan Group comprises early Paleozoic shallow metamorphic marine volcanic–sedimentary formations [26]. The Saishiteng Mountain experiences frequent magmatic activities, with a variety of basic, neutral, and acidic intrusive rocks present in the region. Intermediate to acidic intrusive rocks, including granodiorite and monzonitic granite, are primarily distributed in the Ordovician, Silurian, Carboniferous, Permian, and Triassic periods [25]. Furthermore, alongside the igneous rock formations, the mountain

also features Jurassic clastic rocks with carbonate rocks, as well as Triassic, Carboniferous, and Silurian clastic rocks and carbonate rocks (Figure 1d).

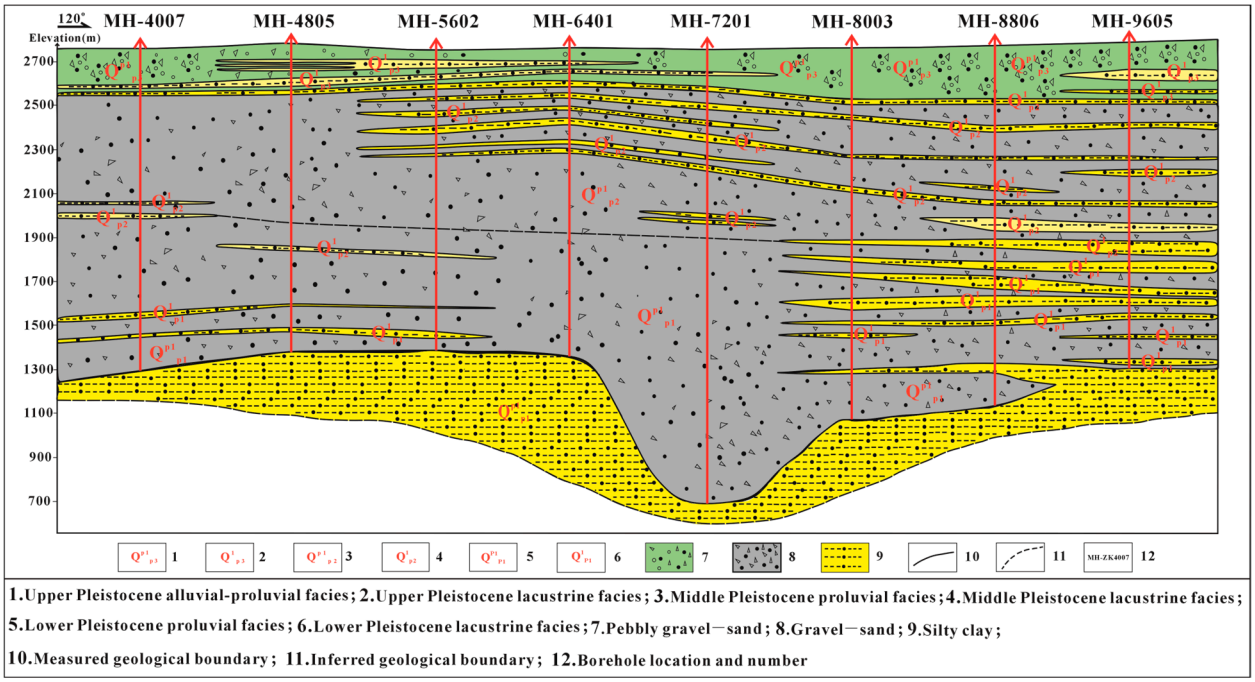


Figure 2. Geological–hydrogeological vertical profile map of the study area.

3. Sampling and Analysis Methods

Samples of sand–gravel brines were collected from the alluvial fan at the base of Saishiteng Mountain in the MHB. To ensure the integrity of the samples, the sand–gravel brines were primarily collected directly from boreholes. After drilling and core extraction were completed, methods such as piston washing were used to clean the boreholes until the water was clear and free of sand. A pumping test was then conducted, followed by sampling. This study focuses on deep gravelly pore brine, and to prevent the influence of shallow water bodies, thicker aquitards were selected between 150 and 300 m in the boreholes to isolate the water. The samples were collected from brine storage strata in alluvial–proluvial facies and lacustrine facies deposited during the Pleistocene to Holocene periods.

During the pumping test, a water sample was collected every 4 h. After rinsing the bottles with distilled water, 1500 mL of the brine was collected and sealed promptly, with the sample number clearly labeled. The collected brine samples were then filtered through a 0.45 μm cellulose acetate filter into pre-cleaned 200 mL bottles. The samples were sent to the Rock and Mineral Testing Center of the Qaidam Comprehensive Geological and Mineral Exploration Institute in Qinghai Province for testing and analysis within 5 days. The deep sand–gravel brines were chemically analyzed for elements such as K^+, Na^+, Ca^{2+}, Mg^{2+}, Li^+, B_2O_3, Cl^-, $SO_4{}^{2-}$, $HCO_3{}^-$, $CO_3{}^{2-}$, and Sr^{2+}, along with measurements for pH, density, and total dissolved solids (TDSs). The concentrations of K^+, Na^+, Ca^{2+}, Mg^{2+}, $SO_4{}^{2-}$, B_2O_3, Li^+, and Sr^{2+} were determined using inductively coupled plasma atomic emission spectroscopy (ICP-AES), while Cl^- was measured using the $AgNO_3$ titration method. The $CO_3{}^{2-}$ and $HCO_3{}^-$ were titrated by HCl with precision less than 0.3%. Each borehole produced dozens of water samples during the pumping tests. The results showed no significant changes in water quality over time during pumping. Therefore, the arithmetic mean of the ion concentrations from each borehole was calculated, providing a more representative average value. The detailed test results are shown in Table 1.

Table 1. K^+ concentrations and characteristic ion coefficients in deep sand–gravel brine of MHP.

Number	Borehole Number	TDSs (g/L)	pH Value	K^+ (g/L)	Na-Cl Coefficient	Ca-Mg Coefficient	Desulfurization Coefficient	K-Cl Coefficient	Cl-I Coefficient	Br-Cl Coefficient	Depth (m)
1	MH-0005	260.04	7.80	0.52	0.86	0.13	1.43	3.32	4.76×10^4	0.17	237–700 m
2	MH-0800	114.69	7.48	0.46	0.86	0.82	1.12	6.68	1.05×10^4	0.37	152–702 m
3	MH-0802	263.92	7.01	2.24	0.86	0.15	1.12	14.08	5.94×10^4	0.16	257–1121 m
4	MH-0808	290.74	7.53	3.28	0.83	0.11	0.95	18.60	10.14×10^4	0.15	207–800 m
5	MH-1609	267.57	7.98	1.51	0.83	0.48	0.39	9.19	2.97×10^4	0.23	219–685 m
6	MH-2413	258.75	7.40	0.83	0.85	0.70	0.34	5.24	3.02×10^4	0.19	164–1500 m
7	MH-3212	256.23	7.26	2.40	0.84	0.29	0.76	15.44	4.28×10^4	0.20	146–803 m
8	MH-4007	257.50	7.38	2.62	0.82	0.25	0.80	17.73	4.85×10^4	0.20	162–1500 m
9	MH-4010	252.92	7.38	2.72	0.83	0.27	0.69	17.69	4.21×10^4	0.24	181–1391 m
10	MH-4802	176.38	7.68	1.34	0.81	0.36	0.85	12.47	2.83×10^4	0.20	235–957 m
11	MH-4805	277.91	7.56	2.70	0.82	0.31	0.46	15.84	4.05×10^4	0.19	190–1435 m
12	MH-5600	242.74	7.63	2.56	0.81	0.32	0.60	17.23	2.79×10^4	0.22	202–1155 m
13	MH-5602	249.51	7.17	2.71	0.80	0.29	0.52	17.74	5.40×10^4	0.20	208–1482 m
14	MH-6400	250.50	7.20	2.11	0.81	0.42	0.50	13.73	2.76×10^4	0.27	250–1254 m
15	MH-6401	272.36	7.29	2.63	0.81	0.51	0.33	15.70	3.00×10^4	0.44	236–1406 m
16	MH-7200	257.56	7.35	2.20	0.81	0.49	0.38	13.90	3.54×10^4	0.21	213–1212 m
17	MH-7201	275.38	7.47	2.31	0.82	0.55	0.29	13.69	2.93×10^4	0.24	268–2066 m
18	MH-8003	271.74	7.57	1.52	0.82	0.83	0.26	9.10	2.10×10^4	0.22	247–1704 m
19	MH-8005	280.23	7.55	1.79	0.82	0.71	0.28	10.37	1.34×10^4	0.25	280–1301 m
20	MH-8805	224.27	7.61	1.43	0.82	0.65	0.37	10.40	2.21×10^4	0.24	266–994 m
21	MH-8806	264.18	7.58	2.13	0.81	0.47	0.38	13.14	3.81×10^4	0.24	295–1695 m
22	MH-9605	132.09	7.55	0.30	0.85	1.01	0.29	3.71	1.79×10^4	0.22	222–1501 m

4. Results

The elemental concentrations of the sand–gravel brines in the MHB are detailed in Table 1. The TDS value of the sand–gravel brines in the MHB ranges from 114.7 to 290.7 g/L, slightly lower than that of the sand–gravel brines of the western QB (276.9 to 311.4 g/L) [7]. Moreover, the TDS value of the sand–gravel brines in the MHB is lower than that of the intercrystalline brines (465 g/L), confined brines (305 g/L), and lake surface brines (456 g/L), yet higher than that of river water (0.05 g/L) and groundwater (10 g/L) [15]. Regarding the content of major cations, the average potassium (K^+) content of the sand–gravel brines in the western QB is 13.8, which is higher than that in the sand–gravel brines (1.9 g/L) in the MHB. This means that the sand–gravel brines in the MHB and western QB exhibit similar characteristics in terms of sodium (Na^+) and chloride (Cl^-) ion content. In the MHB, the Na^+ and Cl^- contents of the sand–gravel brines (Na = 79.9 g/L, Cl = 149.5 g/L) in the front alluvial fan of Saishiteng Mountain are lower than those of the intercrystalline brines (Na = 93.5 g/L, Cl = 159.5 g/L) and confined brines (Na = 94.3 g/L, Cl = 181.4 g/L) in the terminal salt lakes.

As for the content of trace elements, the boron (B) content in the sand and gravel pore brine of the MHB and the western QB is much higher than that of lithium (Li) and strontium (Sr). In the MHB, Li concentrations (2.5 mg/L) are lower than those found in intercrystalline brines (9.51 mg/L) and confined brines (10.92 mg/L), whereas Sr concentrations (71.9 mg/L) exceed those in intercrystalline brines (32.8 mg/L) and confined brines (18.1 mg/L) [13,15].

5. Discussion

5.1. Hydrochemical Characteristics of Sand–Gravel Brines in Mahai Basin

The macroion K^+ content in the deep sand–gravel brines ranges from 0.30 to 3.28 mg/L. The boundary grade of KCl in the brine mine is ≥0.2% to 0.4%, and the industrial grade is ≥0.4% (the demonstration index of the deposit). Apart from the low content of MH-0005, MH-0800, M-2413, and MH-8605, the K^+ content in the drilling holes reached the boundary grade, with some even reaching the industrial grade. The Na^+ content ranges from 38.294 to 94.82 g/L, and the NaCl content exceeds 10% in each hole of the brine mine. The Ca^{2+} content ranges from 1.63 to 76.57 g/L; the Mg^{2+} content ranges from 2.08 to 9.86 g/L, with the grade of $MgCl_2$ in brine ore being above 1%. The Li^+ content ranges from 0.16 to 7.47 mg/L; the Cl^- content ranges from 68,856 to 176,392 mg/L; and the SO_4^{2-} content ranges from 633 to 6051 mg/L. The Sr^{2+} content ranges from 21.87 to 141.42 mg/L; the Rb^+ content ranges from 0.045 to 10.73 mg/L. The TDSs range from 114.69 to 290.74 g/L,

classified as medium-to-high-salinity brine. The pH value of the water body generally ranges from 7.01 to 7.98, indicating weak alkalinity.

After a comprehensive analysis of the ion content data in the deep sand–gravel brines, Table 1 clearly reveals the exploration line direction within approximately 15 km for K^+ and Na^+. The contents of Ca^{2+}, Mg^{2+}, and Cl^- gradually decrease from south to north, while the content of SO_4^{2-} shows a different trend in the alluvial fan facies distribution area (0–72) with a gradual increase from south to north, except for a higher concentration in the lacustrine facies in lines 80–88 in the southeast.

The variation curve of the major ion content from northwest to southeast at the southern margin of Saishiteng Mountain, depicted in Figure 3, illustrates similar trends for K^+ and Mg^{2+}, with higher Mg^{2+} content near lines 0, 24, and 96 and lower content in other regions. In contrast, Ca^{2+} shows an inverse trend to Mg^{2+}, most notably along line 02–88. The overall content of SO_4^{2-} displays a decreasing trend towards the east. The variations in Na^+ and Cl^- contents show a consistent trend, with minimal changes observed along lines 0–88 and a low value exhibited at line 96.

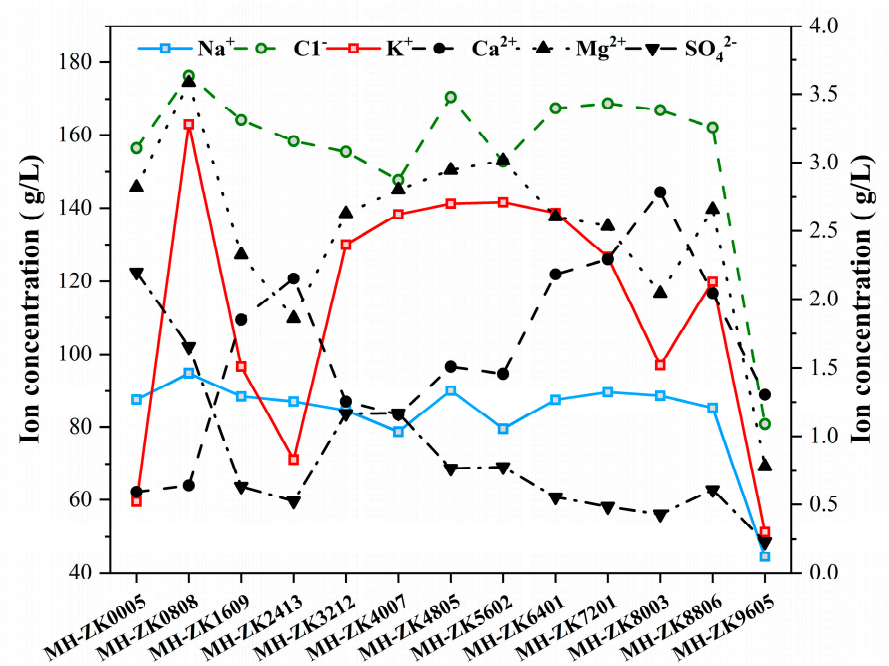


Figure 3. Vertical variation curve of major ion content in deep sand–gravel brine of the Mahai Basin.

After conducting a comprehensive analysis of the sample analysis results in the study area, characteristic coefficients for underground brine were derived as seen in Table 2. The Na/Cl coefficient ranges from 0.80 to 0.86, the Ca/Mg coefficient ranges from 0.11 to 1.01, the desulfurization coefficient ranges from 0.26 to 1.43, the K/Cl series coefficient ranges from 3.32 to 18.60, and the chloro-iodine coefficient ranges from 1.05×10^4 to 10.14×10^4, with all drilling holes except for MH-0808 exhibiting coefficients for chlorine and iodine below 1.00×10^5. The bromo-chlorine coefficient ranges from 0.15 to 0.44.

Table 2. K^+, Na^+, Mg^{2+}/Cl^--H_2O System (25°) Metastable Phase Diagram Index (data from Figure 4).

Figure Point Number	Borehole Number	Hydrochemical Components (mg/L)					Phase Diagram Index (%)		
		K^+	Na^+	Mg^{2+}	$C1^-$	SO_4^{2-}	2KC1	2NaC1	$MgC1_2$
1	MH-4007	2619.02	78,697.87	7706.21	147,783	3205	1.8	81.7	16.4
2	MH-4805	2704.09	90,098.74	8101.42	170,482	2106	1.6	83.4	15
3	MH-5600	2556.83	77,669.73	7414.20	148,611	2403	1.7	82.7	15.7
4	MH-6401	2630.88	87,490.24	7159.56	167,504	1518	1.4	85.7	12.9
5	MH-7200	2197.47	83,295.97	6668.98	158,313	1623	1.4	85.7	12.9

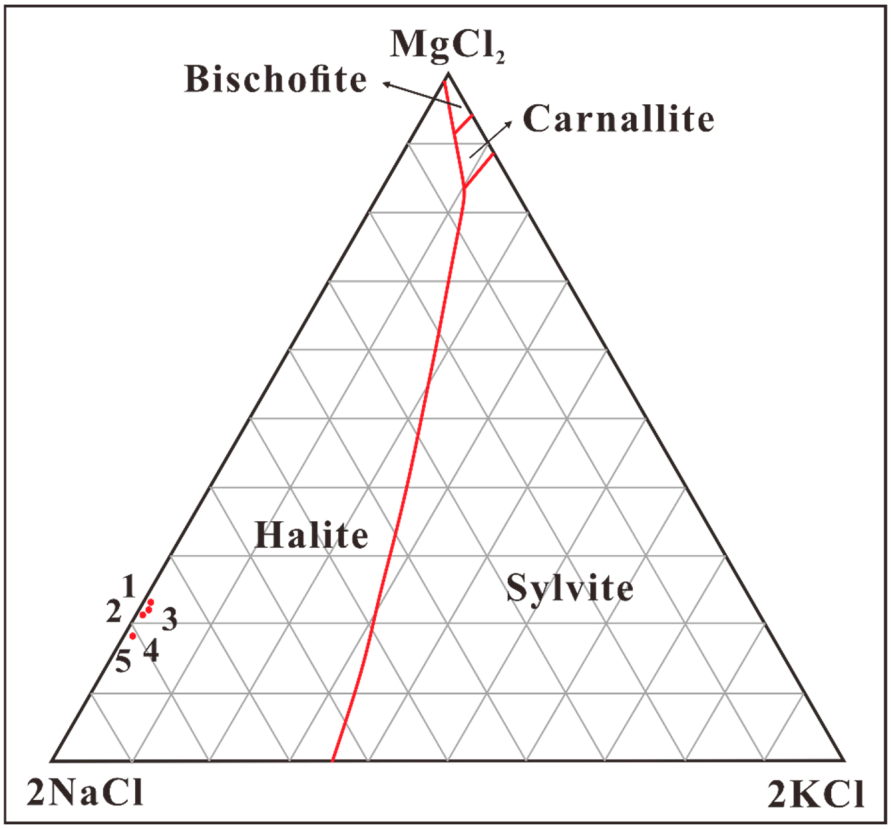


Figure 4. K^+, Na^+, and Mg^{2+}/Cl^--H_2O system (25 °C stability phase diagram).

The abundance and interaction of major ions and cations in deep sand–gravel brines dictate the hydrochemistry of the brine. Different types of brines exhibit corresponding main ion compositions and water–salt equilibrium systems. According to Figure 4, the ion equilibrium system in the study area includes K^+, Na^+, and Mg^{2+}/Cl^--H_2O.

The representative holes MH-4007, MH-4805, MH-5600, MH-6401, and MH-7200 project the samples onto the metastable phase diagram of the quaternary system K^+, Na^+, and Mg^{2+}/Cl^--H_2O at 25 °C (Figure 4). The diagram reveals that the brine is situated in an area of low potassium and magnesium but high sodium, indicative of the crystallization zone for halite minerals, suggesting that the brine type corresponds to a single chlorination type.

5.2. Genesis of Sand–Gravel Brine Deposit in Mahai Basin

5.2.1. Tectonic Evolution and Mineralization of Mahai Basin

The MHB, where the study area is located, lies in the western segment of the subsidence zone of the western part of QB. It is a sub-basin formed by folding and faulting tectonic movements [27]. During the basin's evolution, sedimentary environment changes, and climate fluctuations, the formation of salt deposits occurred. Before the Neogene, the MHB region was part of the ancient Qaidam Lake, continuously receiving input from surrounding water systems rich in saline materials [12]. This sustained deep-lake, shallow-lake, and lakeshore environments (Figure 5a), which facilitated the concentration, the differentiation of brine, and the relative enrichment of potassium. Since the Neogene, the basin has been an intracontinental depression basin under compressional conditions [28]. The Saishiteng Mountain Front Fault, the Lenghu Fault, and other reverse faults in the MHB gradually formed (Figure 5b). From the late Pliocene to the end of the Middle Pleistocene, the uplift of the Lenghu Anticline led to the separation and closure of the MHB from the ancient Qaidam Lake, forming an independent basin [12] (Figure 5c). At that time, the basin had already become a brine lake. The sources of mineralizing

materials included weathered and leached K^+ and other substances, deep-circulating water, and inherited ancient brine from the original paleo-brine lake. During the Early Pleistocene, the MHB region experienced a mild and humid climate with abundant rainfall and strong hydrodynamics [12]. Sediments were predominantly composed of sand and gravel, characteristic of typical alluvial–proluvial facies. This provided ample space for the formation of deep gravelly pore brine deposits. During the Middle Pleistocene, the climate gradually became hotter and drier, leading to the onset of gypsum deposition, with environments dominated by lakeshore and shallow lacustrine facies [12]. By the Late Pleistocene, the climate became extremely arid, significantly reducing the water supply to the MHB [12]. As a result, Mahai Lake gradually shrank, and by the Holocene, the salt lake had completely dried up, forming a wide playa [29]. Meanwhile, under the influence of tectonic movements and geomorphology, the sedimentary center, or lake water, shifted and migrated eastward. This resulted in the formation of the MHB salt lake in the depressions near the water supply sources (Figure 5d).

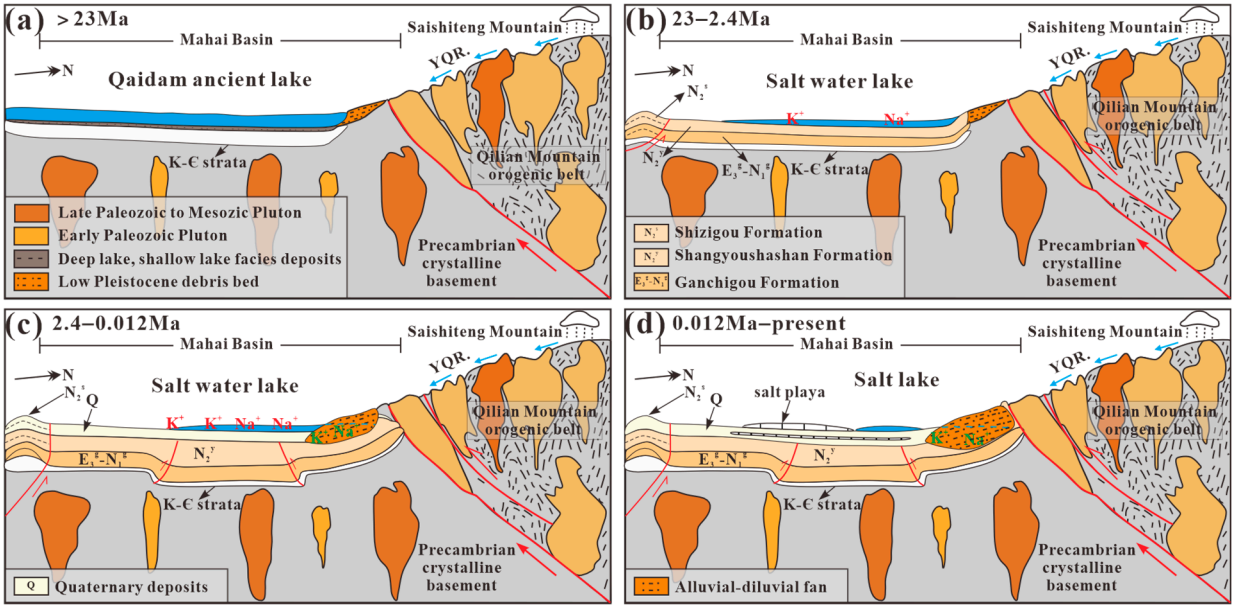


Figure 5. Evolution schematic diagram of salt lakes in the Mahai Basin: (**a**) deep lake, shallow lake, and lacustrine environments in the Mahai area before the Neogene; (**b**) the Saishiteng Mountain Front Fault, Lenghu Fault, and other thrust faults in the Mahai Basin gradually formed; (**c**) from the end of the Pliocene to the end of the Middle Pleistocene, with the uplift of the Lenghu Anticline, the Mahai Basin became separated and enclosed from the ancient Qaidam Lake; (**d**) controlled by tectonic movements and landforms, the sedimentary center, i.e., the lake, shrank and migrated eastward, forming the Mahai Salt Lake in a depression close to the recharge source.

5.2.2. Genetic Analysis of K-Rich Sand–Gravel Brine

This study systematically analyzed the hydrochemical characteristics of deep sand–gravel brines in the alluvial–proluvial zone at the piedmont of Saishiteng Mountain. By comparing the ionic characteristics and isotopic compositions (δD, $\delta^{18}O$, $\delta^{37}Cl$, and $\delta^{7}Li$) with intercrystalline brines and confined brines from the southern depressions, the formation mechanism of this newly discovered brine deposit was revealed [11,13,15].

Based on the main ion concentration variations shown in Table 1 and Figure 3, there is a gradual decrease in the concentrations of K^+, Na^+, Ca^{2+}, Mg^{2+}, Cl^-, and TDSs in the brine from south to north along the exploration direction. This suggests that there is horizontal zonation of the ion concentrations in the deep sand–gravel brines from lacustrine facies in the depressions towards alluvial–proluvial facies in the piedmont. It indicates the migration direction of ions within the brine. Vertically, within the 15 km zone surrounding Saishiteng Mountain, the variation trends of K^+ and Mg^{2+} are generally consistent, while Na^+ and

Cl^- exhibit a similar trend. This suggests horizontal zonation of ions within the brine. The opposite trends of Ca^{2+} and Mg^{2+}, particularly evident along the 02–88 line, are likely due to gypsum precipitation during the evaporation and migration of brine, leading to a significant reduction in Ca^{2+} and an increase in Mg^{2+} ($Ca^{2+} + MgSO_4 = CaSO_4\downarrow + Mg^{2+}$). This observation aligns with the presence of small amounts of gypsum mineral in the Middle Pleistocene alluvial–proluvial gravel layers in the northern region.

According to Table 2, the Na/Cl ratio in the deep brine of the study area ranges from 0.80 to 0.86, which is similar to the intercrystalline brines in the southern depressions (Na/Cl ratio of 1.0), indicating residual evaporative brine characteristics. The Br/Cl ratio generally ranges from 0.15 to 0.27, with lower values approaching those of intercrystalline brines (0.1), while higher values are closer to evaporite leaching brines (0.33 or less). The Br/Cl ratios in boreholes MH-0800 and MH-6401 are 0.37 and 0.44, respectively, which are closer to metamorphic brine values (>0.33), suggesting a multi-source brine characteristic. The Ca/Mg ratio reflects the degree of metamorphism in formation water; the longer the water has been present and the better its confinement, the higher the degree of metamorphism and the higher the Ca/Mg ratio. The Ca/Mg ratio of the deep sand–gravel brines in this area ranges from 0.11 to 1.01, indicating that the sand–gravel brines have a relatively short formation time, poor confinement, and a low degree of metamorphism. The desulfurization coefficient reflects the degree of confinement of formation water, with smaller values indicating less confinement. The desulfurization coefficient of the deep sand–gravel brines in this area ranges from 0.26 to 1.43, which is far higher than that of intercrystalline brines (0.08) but much lower than anticlinal brines (10.67), further indicating that the deep sand–gravel brine in this area has poor confinement. Closer to the piedmont of Saishiteng Mountain, the desulfurization coefficient increases, reflecting thinner and more unstable aquitards (clay or sandy clay) and showing evidence of surface freshwater influence.

The deep sand–gravel brines are enriched in Na^+ and Cl^- ions, while depleted in SO_4^{2-} and HCO_3^- ions, with CO_3^{2-} ion concentrations being negligible. The TDSs range from 114.69 to 290.74 g/L, and the combined Na^+ and Cl^- ions account for more than 90% of the TDSs. In the K^+, Na^+, and Mg^{2+}/Cl^--H_2O quaternary metastable phase diagram, the hydrochemical type of the water is consistently of the chloride type. The intercrystalline brines and confined brines in the southern DZMH Lake depression exhibit low-K and high-Na characteristics, with most of the water types being magnesium Cl-SO_4 and some being chloride types. The analysis of the geological characteristics of the K-bearing brine strata in the deep sand–gravel brines of the alluvial–proluvial fan and the intercrystalline brines and confined brines in the southern depressions suggests that the sand–gravel brine reservoirs of the alluvial fan are directly connected to the terminal salt lakes and underground brine. Shallow intercrystalline brines or confined brines may be recharged into deeper gravel reservoirs due to topographical differences, indicating a hydraulic and intrinsic genetic relationship between the two.

The H-O, Cl, and Li isotopes in saline mineral deposits are important indicators for determining the source of materials [11]. The δD values of the sand–gravel brines in the MHB range from −56.9‰ to −17.6‰, and $\delta^{18}O$ values range from −5.70‰ to +6.00‰ (Figure 6). These isotopic signatures are scattered to the right of the local meteoric water line (LMWL) in the "Saishiteng Mountain-Alluvial Fan-Salt Lake" system, indicating that the sand–gravel brines receive hydrological recharge from atmospheric precipitation and have undergone significant evaporation and concentration. The $\delta^{37}Cl$ values (−0.26‰ to +0.25‰) and δ^7Li values (+33.84‰ to +43.82‰) of the deep sand–gravel brines in the alluvial–proluvial fan are comparable to those of the intercrystalline brines in the MHB [11], revealing similar geochemical characteristics between the sand–gravel brines and intercrystalline brines.

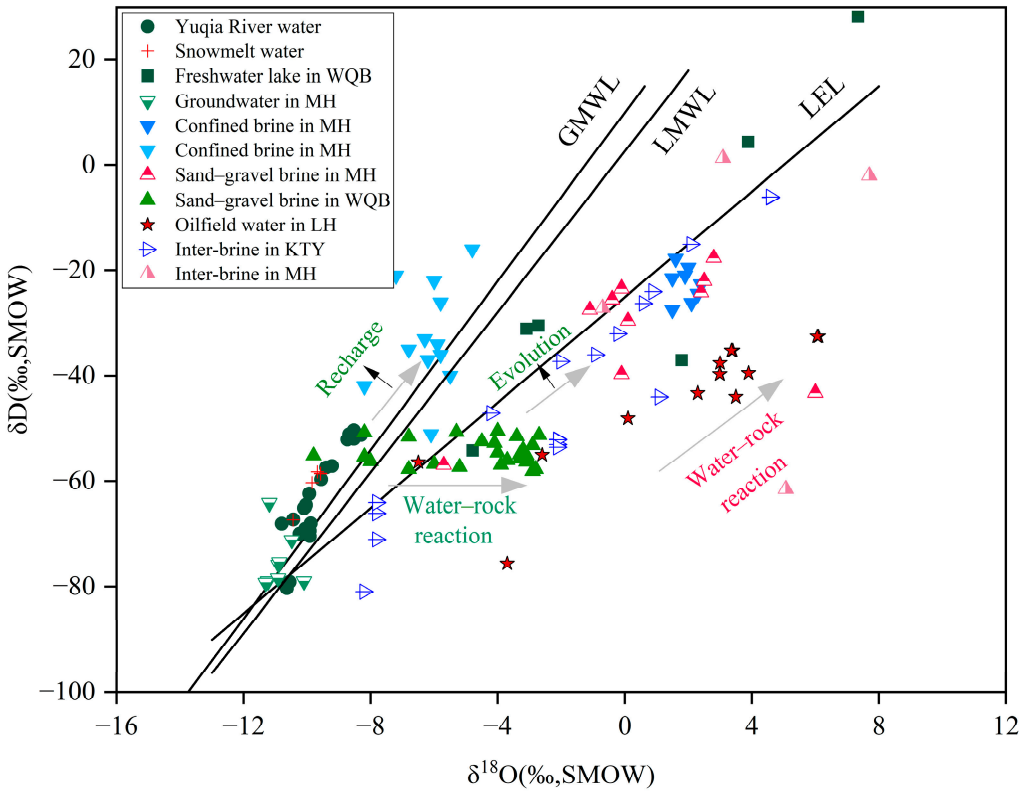


Figure 6. Hydrogen and oxygen isotopes of brines and surrounding water in the Mahai Basin. Data source: Yuqia River water and snowmelt water from [29]; lake water from [4]; inter-brine (intercrystalline brine) from [12,30]; confined brines (dark blue triangle) from [15]; confined brines (light blue triangle) from [12]; sand–gravel brines (red triangle) from [11]; sand–gravel brines (green triangle) from [7]; oilfield waters from [9]; and inter-brine (intercrystalline; hollow blue triangle) from [17]. WQB: the western Qaidam Basin (including Dalangtan Basin, Heibei Basin, Chahansilatu Basin, Kunteyi Basin, and Mahai basin); MH: Mahai Basin; LH: Lenghu; KTY: Kunteyi Basin. GMWL: global meteoric water line (GMWL, $\delta D = 8 \times \delta^{18}O + 10$) [4,30]; LEL: the evaporation line of Qaidam Basin (LEL, $\delta D = 5 \times \delta^{18}O - 25$) [7]; LMWL: local meteoric water line (LMWL, $\delta D = 7.6 \times \delta^{18}O + 2.6$) [31].

5.2.3. Genesis of Sand–Gravel Brine Deposit in Mahai Basin Area

The main water sources for the MHB are the surface water system, consisting of the Yuqia River, Naoer River, and Aolao River, which originate in the Qilian Mountain system, as well as groundwater. The water supply for the sand and gravel pore brine reservoir in the MHB is replenished via a thrust fault in the northern QB, serving as a migration pathway. As surface runoff and groundwater transport the byproducts of weathering and forest filtration to the salt lake, the salt lake brine undergoes evolution under arid climate conditions. The coefficients for sodium chloride range from 0.80 to 0.86, while those for bromine chloride range from 0.15 to 0.44 (Table 1). The findings indicate that the deep sand–gravel brines in the MHB are primarily evaporated residual brine, exhibiting characteristics of both salt karst brine and sedimentary brine with multiple origins. The ratios of C_{Na}/C_{Cl}, $\delta^{37}Cl$, and $\delta^{7}Li$ in sand–gravel brines [11], along with Li values and intercrystalline brines and confined brines in the MHB, indicate uniformity. Both types demonstrate similar geochemical traits, supporting the credibility of this newly discovered brine formation. Subsurface brine (intercrystalline brines and confined brines) recharge occurs in the basin, with sand–gravel brines in the alluvial–diluvial fan reservoir connecting with terminal salt lake and underground brines. Shallow intercrystalline brines or confined brines may traverse the topography to replenish deeper sand and gravel reservoirs in various directions.

As a secondary basin within the context of the QB "high mountain and deep basin", the MHB holds significant importance [31]. Its evolution has been shaped by neotectonic movements on the Qinghai–Tibet Plateau. During the early Pleistocene, the climate in the MHB region was mild and humid, characterized by ample rainfall that collected in the frontal depression area of Saishiteng Mountain. As the Middle Pleistocene period approached, the climate transitioned to a drier and hotter phase due to the Middle Pleistocene Climate Transition event (MPT) and the continued plateau uplift. The uplift of the Lenghu anticlinal structure divided the MHB, isolating it from the ancient Qaidam Lake. This process involved the uplift of the southern foothills of the northern Qilian Mountains, exposing bedrock and Paleogene–Neogene strata and leading to intensified denudation and the accumulation of significant detrital deposits that formed numerous pores in the present Saishiteng Mountain area. Simultaneously, as atmospheric precipitation previously gathered in the southern depression evaporated and concentrated in the increasingly arid climate, evaporation salts began to deposit on the lake surface, giving rise to intercrystalline brines and confined brines. With the uplift of the anticline of the lower Lenghu structure, the depositional center shifted northward, where halite had previously been deposited by evaporation and concentration. As a result of this northward movement of the depositional center, intercrystalline brines and confined brines flowed back into the alluvial plains in front of Saishiteng Mountain, forming fan groups. There, the inherited solutions from intercrystalline brines and confined brines accumulated and transformed into deep K-bearing sand–gravel brine deposits.

6. Conclusions

In this study, the concentrations of major and trace elements in the sand–gravel brines in the MHB were systematically analyzed. By integrating the analysis of characteristic coefficients, phase diagrams, and salt evolution trends of sand–gravel brines, a comprehensive examination of the characteristics and origins of the brine is conducted. The key findings are follows:

(1) The major elements of K, Na, Ca, and Cl are highly concentrated in the sand–gravel brine within the Mahai Basin, with K^+ levels ranging from 0.30 to 3.28 g/L. In most boreholes, the K^+ concentration exceeds the boundary grade (KCl boundary grade $\geq$ 0.2–0.4%, K^+ > 2.6 g/L). The Na^+ content ranges from 38.29 to 94.82 g/L, while the Ca^{2+} content is between 1.63 and 76.57 g/L. Additionally, the Sr^{2+} concentration falls within the range of 21.87 to 141.42 mg/L.

(2) After analyzing the phase diagram and salt evolution pattern of sand–gravel brines in the Mahai Basin, it was determined that the metastable phase diagram in the K^+, Na^+, and Mg^{2+}/Cl^--H_2O (25 °C) quaternary system is situated in the low-potassium, magnesium, and high-sodium region, indicating the crystallization zone of halite minerals. This demonstrates that the brine type is Na-Cl type.

(3) The deep sand–gravel brines in the MHB originate from atmospheric precipitation, with ore-forming materials deriving from diverse sources and exhibiting characteristics of residual evaporated brine, in conjunction with salt karst filtration and sedimentary brine.

(4) The genesis of the deep sand–gravel brine deposits in the MHB results from a combination of basin tectonic evolution, brine migration, enrichment, and other controlling factors. It is inferred that the MHB gradually separated from Qaidam Lake from the late Pliocene to the end of the Middle Pleistocene. The basin inherited K^+ ions from ancient brines, which were released due to weathering and leaching of the original paleolake water under arid climatic conditions. Evaporation and infiltration in the lake basin depression initiated the deposition of evaporative salts on the lake surface, leading to the formation of intercrystalline brine and deep confined brine. The sand–gravel brine reservoir located in the frontal alluvial fan of the Saishiteng Mountain interacted with the uplift of the Lenghu Anticline structure, causing the depositional center to shift northward. The pre-existing intercrystalline brines and

confined brines might recharge the northern sand–gravel reservoir through topographical differences, culminating in the formation of deep brine deposits at the front of Saishiteng Mountain.

Supplementary Materials: The following supporting information can be downloaded at: https://www.mdpi.com/article/10.3390/w16243562/s1, Table S1: Stratigraphic overview of the Mahai Basin.

Author Contributions: H.B. (Hongkui Bai) collected samples, experiments, data analysis, and writing. T.P. performed project design, discussion, and revision. G.H. helped with discussion, sample collection and writing. Q.F. helped with discussion. Q.M. and H.B. (Haiyi Bu) carried out the discussion, revision, and sample collection. All authors have read and agreed to the published version of the manuscript.

Funding: This work was supported by the Key Research and Development Plan Project of China (Grant No. 2022YFC2904301).

Data Availability Statement: Data is contained within the article.

Acknowledgments: We thank Tianyuan Chen, Qingkuan Li, Haotian Yang, and Min Li for their help in the sampling and their helpful suggestions in the preparation of manuscript.

Conflicts of Interest: The authors declare that there are no known financial conflicts of interest or personal relationships that could have influenced the work reported in this paper.

References

1. Zheng, M.P.; Yuan, H.R.; Zhang, Y.S.; Liu, X.F.; Chen, W.X.; Li, J.S. Regional distribution and prospects of potash in China. *Acta Geosci. Sin.* **2010**, *84*, 1523–1553. (In Chinese)
2. Zheng, M.P.; Hou, X.H.; Yu, C.Q.; Li, H.P.; Yi, W.H.; Zhang, Z.; Deng, X.L.; Zhang, Y.S.; Guo, T.W.; Wei, Z.; et al. The leading role of salt formation theory in the breakthrough and important progress in potash deposit prospecting. *Acta Geosci. Sin.* **2015**, *36*, 129–139. (In Chinese)
3. Zheng, M.P.; Qi, W.; Zhang, Y.S. Present situation of potash resources and direction of potash search in China. *Geol. Rev. J.* **2006**, *11*, 1239–1246. (In Chinese)
4. Zhang, P.X. *Salt Lake in Qaidam Basin*; Science Press: Beijing, China, 1987. (In Chinese)
5. Li, H.P.; Hou, X.H.; Zheng, M.P.; Fan, F.; Liu, X.C.; Wang, S.L. Discussion on metallogenic model and prospecting direction of Pleistocene gravel brine Potassium deposit in the western Qaidam Basin. *J. Lake Sci.* **2022**, *3*, 1043–1054.
6. Yu, S.Y.; Li, S.Z.; Zhang, J.X.; Peng, Y.B.; Somerville, I.; Liu, Y.J.; Wang, Z.Y.; Li, Z.F.; Yao, Y.; Li, Y. Multistage anatexis during tectonic evolution from oceanic subduction to continental collision: A review of the North Qaidam UHP Belt, NW China. *Earth-Sci. Rev.* **2019**, *191*, 190–211. [CrossRef]
7. Liu, X.X.; Yue, X.; Yu, X.L.; Ma, Z.; Lu, L.; Zhang, X.D.; Ma, Z.D. Characteristics and genesis of the double potash layer metallogenetic model of Kunteyi Depression in the northwest margin of Qaidam Basin. *J. Lake Sci.* **2020**, *1*, 246–258.
8. Li, H.P.; Zheng, M.P.; Hou, X.H.; Sun, B.T.; Liu, G.T.; Dou, Q.C. Hydrochemistry characteristics and origin of new brine sandy gravel in early Pleistocene of Heibei concave in Qaidam Basin. *Earth Sci.* **2014**, *10*, 1433–1442.
9. Fan, Q.S.; Han, G.; Chen, T.Y.; Bai, H.K.; Liu, J.B.; Miao, Q.; Zhang, X.D.; Yang, H.T.; Li, Q.K. Inheritance recharge of subsurface brine constrains on formation of K-bearing sand-gravel brine in the alluvial fan zone of mountain-basin system on the Qinghai-Tibet Plateau. *J. Hydrol.* 2024, *under revise*.
10. Wei, X.J.; Qiang, J.X.; Wang, M.L. Sedimentary characteristics of Quaternary and evolution of saline lake of Mahai potash deposit. *Geol. Qinghai* **1993**, *1*, 40–52. (In Chinese)
11. Song, H.L.; Fan, Q.S.; Li, Q.K.; Han, G.; Chen, T.Y.; Yang, H.T.; Wei, Q. Ca-high water recharge and mixing constrain on evolution and K enrichment of brine deposits in the evaporite basin: Case and analogue study in the Qaidam Basin, Qinghai-Tibet Plateau. *J. Hydrol.* **2024**, *632*, 130883. [CrossRef]
12. Xiang, H.L.; Fan, Q.S.; Li, Q.K.; Du, Y.S.; Han, G.; Liu, J.B.; Bai, H.K. Source and sedimentation of boron deposits in Mahai Basin on the northern Qinghai-Tibet Plateau: Clues from hydrochemistry and B isotopes. *Aquat. Geochem.* **2024**, *30*, 143–161. [CrossRef]
13. Yang, F.; Fan, Q.; Han, G.; Wang, W.; Liu, J.; Bai, H. Origin and Evolution of Deep K-Rich Confined Brine in Mahai Basin, Qinghai–Tibet Plateau. *Aquat. Geochem.* **2024**, *30*, 239–258. [CrossRef]
14. Tan, H.; Rao, W.; Ma, H.; Chen, J.; Li, T. Hydrogen, oxygen, helium and strontium isotopic constraints on the formation of oilfield waters in the western Qaidam Basin, China. *J. Asian Earth Sci.* **2011**, *40*, 651–660. [CrossRef]
15. Li, W.X.; Zhang, X.Y.; Miao, W.L.; Li, Y.S.; Tang, Q.L.; Wang, P.; Li, Y.; Zhu, G.Q. Hydrochemical characteristics of Oilfield Waters in Lenghu No 3, Structure Area of North Edge of Qaidam Basin. *J. Salt Lake Res.* **2016**, *24*, 12–18. (In Chinese)
16. Fan, Q.; Lowenstein, T.K.; Wei, H.; Yuan, Q.; Qin, Z.; Shan, F.; Ma, H. Sr isotope and major ion compositional evidence for formation of Qarhan Salt Lake, western China. *Chem. Geol.* **2018**, *497*, 128–145. [CrossRef]

17. Hu, S.Y.; Zhao, Q.S.; Wang, G.C.; Zhang, J.W.; Feng, J. Hydrochemical dynamic characteristics and evolution of underground brine in the Mahai Salt Lake of the Qaidam Basin Qinghai-Tibet Plateau. *Acta Geol. Sin.* **2018**, *5*, 1981–1990. [CrossRef]
18. Li, J.; Li, T.; Ma, Y.; Chen, F. Distribution and origin of brine-type Li–Rb mineralization in the Qaidam Basin, NW China. *Sci. China Earth Sci.* **2022**, *65*, 477–489. [CrossRef]
19. Wang, Z.Q.; Hu, X.M.; Wu, Y.B.; Wang, C.Y. Sedimentology and evolution of sedimentary facies for the Cenozoic in the Mahai Region on the Northern Margin of the Qaidam Basin. *Acta Geol. Sin.* **2011**, *30*, 129–131.
20. Hu, S.Y.; Zhao, Q.S.; Ma, J.Y. Hydrochemical characteristics of confined brine in Mahai potash area in Qinghai province. In *Water Resources and Environment, Proceedings of the 2015 International Conference on Water Resources and Environment, Beijing, China, 25–28 July 2015*; CRC Press: Boca Raton, FL, USA, 2016; pp. 17–25.
21. Lowenstein, T.K.; Spencer, R.J.; Zhang, P.X. Origin of ancient potash evaporites: Clues from the modern nonmarine Qaidam Basin of western China. *Science* **1989**, *245*, 1090–1092. [CrossRef]
22. Zhang, P.X.; Zhang, B.Z.; Lowenstein, T.K.; Spencer, R.J. *Origin of Ancient Potash Evaporites: Examples from the Formation of Potash of Qarhan Salt Lake in Qaidam Basin*; Science Press: Beijing, China, 1993.
23. Zhou, Y.L. Geological and Geochemical Characteristics and Tectonic Evolution of Tanjianshan Group in the Saishiteng Mountain, Northern Margin of Qaidam Basin. Ph.D. Thesis, Chang'an University, Xi'an, China, 2021.
24. Zhuang, Y.J.; Peng, X.; Zhou, Y.L.; He, S.P.; Wang, P.L.; Wang, L.X. Genesis and geological significance of late ordovician Nb-rich basalts from Tanjianshan Group in Saishitengshan Mountain, Northern Margin of Qaidam Tectonic belt. *Northwest Geol.* **2023**, *56*, 63–80.
25. Lu, S.N.; Wang, H.C.; Li, H.K. Redefnition of the "Dakendaban Group" on the Northern margin of the Qaidam basin. *Geol. Bull. China* **2002**, *21*, 19–23.
26. Wang, L.X.; He, S.P.; Zhuang, Y.J. Discussion on newly disintegrated metavolcanic rock series from the Dakendaban Group in Xiaosaishiteng Mountain Area, Qinghai Province. *Northwest Geol.* **2022**, *55*, 1–18.
27. Wang, Y.H. Research on Sedimentary Environment of Mohair Salt Lake in Quaternary in the Qaidam Basin Qinghai Province. Master's Thesis, University of Geosciences, Beijing, China, 2016.
28. Jin, Z.J.; Li, J.C.; Tang, L.J.; Yu, Y.X.; Jiang, B.; Zhang, M.L.; You, F.B.; Zhang, B.S. Cenozoic Wave Processes and Their Relationships to Hydrocarbon in the Qaidam Basin. *Acta Geol. Sin.* **2006**, *3*, 359–365.
29. Zhu, P.C. Groundwater Circulation Patterns of Yuqia-Mahai Basin in the Middle and Lower Reaches of Yuqia River. Ph.D. Thesis, Jilin University, Changchun, China, 2015. (In Chinese)
30. Craig, H. Isotopic variations in meteoric waters. *Science* **1961**, *133*, 1702–1703. [CrossRef] [PubMed]
31. Yuan, J.Q.; Huo, C.Y.; Cai, K.Q. The High Mountain—Deep Basin Saline Environment—A New Genetic Model of Salt Deposits. *Geol. Rev.* **1983**, *2*, 159–165.

Disclaimer/Publisher's Note: The statements, opinions and data contained in all publications are solely those of the individual author(s) and contributor(s) and not of MDPI and/or the editor(s). MDPI and/or the editor(s) disclaim responsibility for any injury to people or property resulting from any ideas, methods, instructions or products referred to in the content.